

Article – Engineering, Technology and Techniques

Analysis of Complementarity between Renewable Sources in River Basins: a Proposed Methodology and a Brazilian Case Study

Camila de Oliveira Dias^{1*}

<https://orcid.org/0000-0003-4059-7051>

Elder Vicente de Paulo Sobrinho²

<https://orcid.org/0000-0001-7735-6732>

Ivan Nunes Santos¹

<https://orcid.org/0000-0001-8630-1354>

¹Universidade Federal de Uberlândia, Faculdade de Engenharia Elétrica, Uberlândia, Minas Gerais, Brasil;

²Universidade Federal do Triângulo Mineiro, Faculdade de Engenharia Elétrica, Uberaba, Minas Gerais, Brasil.

Editor-in-Chief: Alexandre Rasi Aoki

Associate Editor: Alexandre Rasi Aoki

Received: 18-Mar-2024; Accepted: 04-Jul-2024

*Correspondence: camiladeoliveiradias@hotmail.com; Tel.: +55-34992323935 (C.O.D.).

HIGHLIGHTS

- A methodology for analyzing complementarity between renewable sources is proposed.
- The complementarity between sources for a Brazilian river basin is analyzed.
- Analysis of complementarities in hydraulic generation with wind and solar sources.
- Results using Spearman's coefficient and Kendall's tau are presented.

Abstract: Exploring the natural complementarity that exists between renewables is pivotal for optimizing clean electricity generation. Quantifying this complementarity can enhance electrical planning, reducing waste of natural resources and guiding investment decisions more effectively. To quantify the complementarity existing in Brazilian river basins, a methodology was proposed. Data on influent natural energy, irradiance, and wind speed are analyzed using Python. Through a comprehensive process, the most suitable correlation coefficient is identified. The subsequent calculation of coefficients for specific source combinations and periods, as well as the application of the Innovative Trend Analysis methodology, allow an understanding of the existing complementarity dynamics. The methodology was applied to the Capivari River basin, located in the state of Paraná, which included a monthly analysis of complementarity between hydraulic generation with wind and photovoltaic sources from June 2016 to April 2024. There was no discrepancy in the interpretations of the results obtained for Spearman's Rho and Kendall's Tau, although the magnitude of Kendall's Tau is, on average, 30% lower for the combination of photovoltaic and hydraulic and 49% for the combination of wind and hydraulic. The combination of wind and hydraulics exhibited seasonal complementarity, demonstrating lesser advantages compared to photovoltaic generation, with around 61% of the acquired values of Spearman's Rho being negative, approximately 28% of which were negligible. This percentage is lower than the over 82% of negative values observed for the photovoltaic and hydraulic combination, of which 12% are negligible. The results are consistent with the literature and validate the proposed methodology.

Keywords: Brazilian case study; complementarity; correlation coefficients; renewable energy sources; river basin.

INTRODUCTION

The imperative to mitigate greenhouse gas emissions has spurred a progressive surge in renewable energy generation. Nonetheless, inherent characteristics, notably the intermittency in solar, wind, and sea wave processes resulting from their reliance on variable conditions, pose significant challenges and complexities [1]. To overcome this challenge, some alternatives can be applied, such as: the use of energy storage systems, the interconnection of geographically distributed generators, the strategic management of load dispatch, and the integration of electric vehicles as distributed sources, particularly in microgrids. Other solutions involve the use of sources with a high level of complementarity, and also plant hybridization processes [2–4].

In this context, complementarity refers to the capacity of one or more sources to provide energy in a manner that complements each other, either temporally, spatially, or both. This ensures that the power generated by one source complements that of another, and their combined output is sufficient to fulfill the demand of the connected load. Temporal complementarity is a characteristic of two or more types of sources that complement each other over time in the same region. For example, in the case of two sources, the minimum availability of one coincides with the maximum availability of the other. This dynamic complements the global energy supply and can be better utilized with the use of hybrid systems [1,5–7]. Spatial complementarity, on the other hand, refers to the complementarity between generations located in different regions. This characteristic is useful for better management of interconnected systems and should be considered in electrical planning [6].

In cases where studies indicate the existence of complementarity between solar and hydraulic generations for a given region, for example, there is the possibility of installing floating photovoltaic systems on the reservoirs of hydroelectric plants. In this way, in addition to increasing energy production and controllability, considering that hydroelectric generation is capable of responding to the natural fluctuation of photovoltaics [8], several other benefits can be listed. Among them, benefits include the increase in system efficiency due to the evaporative cooling of panels and cables caused by the body of water. Additionally, there is the reduction in evaporation of the free water surface, which helps to preserve the volume of water stored. Further benefits are the reduction in the formation of waves and consequently erosion on the banks of the reservoirs, the sharing of transmission infrastructure that does not require greater investment, and the use of the reservoir without the need to occupy new areas. Lastly, the approach facilitates the sharing of maintenance and operation labor [9]. This strategy not only enhances energy generation but also optimizes the utilization of the country's water potential, aligning with the recent efforts aimed at increasing energy diversity while minimizing environmental impact [10]. Nevertheless, despite the numerous advantages, there are drawbacks that must be considered in comparison with land-based systems. These disadvantages may or may not be offset by the advantages mentioned, such as higher costs of project, initial installation, and maintenance, as well as environmental impacts such as changes in water quality and disruption of wildlife.

The significant benefits and abundant renewable potential in Brazilian territory justify the growing interest in complementarity. Studies focusing on specific regions within Brazil to assess the complementarity between energy sources have been published [5,6,8,9,11–21]. However, while these studies provide valuable insights, they often focus on broader regional analyses or combinations of two energy sources. A notable gap remains in the literature regarding detailed studies that simultaneously assess the complementarity between hydraulic and photovoltaic, as well as hydraulic and wind source within a single river basin. This discrepancy is further evidenced by the importance of hydraulic generation for the Brazilian electrical matrix, which represents more than 50% of the national installed capacity [22]. To address this gap, we propose a method for assessing temporal complementarity within Brazilian river basins defined by the ONS (National Electric System Operator). Subsequently, a case study is conducted to evaluate the complementarities between hydraulic, photovoltaic, and wind generation within the Capivari River basin, in the state of Paraná. This study includes a comparison of the results obtained using different metrics, thereby providing a detailed and localized understanding of energy complementarity.

In numerical terms, the complementarity between two renewable energy sources can be computed through correlation coefficients or complementarity indices, which consider their typical variations and availability over a pre-defined period. In a simplified way, a correlation coefficient measures the degree of relationship between two variables, reflecting the strength and direction of their association. In the field of renewable energy research, the most widely cited coefficients for evaluating the correlation between renewable resources are Pearson, Kendall, and Spearman [1,23,24].

The vast majority of researchers use Pearson's coefficient as a metric when seeking to quantify the complementarity between renewable sources in their articles, such as [12,13,19,25–32]. Pearson's coefficient is indeed more efficient when data adheres to a normal distribution; however, the statistical efficiency of Kendall and Spearman's coefficients remains above 70% for all possible values of the population correlation, as noted in [33]. Nevertheless, the Pearson coefficient, being a parametric measure, is a most suitable for the linear relationship between two variables and may not be the best choice when the data does not follow a normal distribution. Moreover, in many instances, researchers do not verify or explicitly mention the data distribution before computing the Pearson coefficient [12,19,25–32]. In addition to normality, Pearson's coefficient also assumes linearity and homoscedasticity of the dataset [34].

Therefore, the proposed method diverges from existing literature in that it incorporates statistical tests that provide information about the distribution of data. Based on this information, it is possible to determine which coefficient should be used in each case. The evaluation will also encompass potential discrepancies between the results of different coefficients applied. When the assumptions for applying the Pearson coefficient are not met, other alternatives are utilized, such as Spearman's Rank, also known as the Spearman's Rho (ρ_s) and Kendall's Tau (τ) [35]. These are non-parametric methods, which are worthwhile as they do not require prior knowledge of the data's distribution. In practice, many real-world data sets do not conform to a specific distribution model. Consequently, non-parametric approaches are flexible and suitable for such data [36]. Furthermore, non-parametric correlation measures are robust to outliers, adding to their practical utility [33].

In addition to these traditional methods, we introduce the Innovative Trend Analysis (ITA) methodology with significance test as an innovative approach for assessing energy complementarity. This method is among the modern trend analysis techniques. It is widely used to investigate issues related to meteorological data, such as precipitation trends under varying conditions [37–40]. Nevertheless, it had not yet been employed as a metric for assessing energy complementarity [1,24].

ITA allows for a more comprehensive evaluation by identifying and analyzing trends and patterns within the data that may not be evident through conventional correlation coefficients. This methodology not only considers linear and non-linear relationships but also incorporates adaptive mechanisms to account for temporal variations and external influencing factors. The application of ITA in renewable energy studies provides a robust framework to understand the intricate dynamics between different energy sources, offering deeper insights and potentially enhancing the accuracy of complementarity assessments. This novel approach addresses the limitations of conventional methods, offering a more detailed and flexible analysis suitable for the complex nature of renewable energy data [41]. For example, studies have shown that hydro-climatological time series may contain characteristics of past changes in terms of climate variability, including shifts, cyclic fluctuations, and more significantly, trends. ITA is based on non-parametric methods without restrictive assumptions, providing objective and quantitative trend identification applicable to various types of time series [39,42].

METHODOLOGY

The proposed methodology is characterized by the possibility of application in any of the Brazilian river basins defined by ONS. This section delineates the entire procedure, encompassing the process from data acquisition to obtaining results. To apply the methodology, the Python programming language was used. In addition to being a very useful tool for data analysis, it is a simple and intuitive language, facilitating both code composition and comprehension. An additional benefit lies in the extensive array of freely available resources, like libraries with different purposes. All these benefits make Python one of the most popular languages today, according to the TIOBE ranking [43], which analyzes data from searches in online search tools and posts made by developers in specialized forums [44].

Data Acquisition

The complementarity analysis was carried out based on the results obtained for the correlation coefficients. To calculate these coefficients, the study utilized daily ENA (Affluent Natural Energy) data, which is measured as storable in daily average power (MWavg) of the river basins. These data are made available by the ONS. Additionally, meteorological data were used, provided by INMET (Brazilian National Institute of Meteorology) and accessed through the BDMEP (Meteorological Data Bank). This database contains daily meteorological data in digital form from historical series from several stations, and is maintained in accordance with the international technical standards of the World Meteorological Organization [45].

The network of automatic meteorological stations (AMSs) operated by INMET is the most comprehensive data collection network in Brazilian territory [46]. Files are available in CSV format with hourly data for each

AMS over a period of one year. Data can be queried from the year 2000 onwards. However, it is important to note that the start date of operation for several stations is later, resulting in a smaller dataset for those locations. In each file, the following station location data are provided: region, federative unit, latitude, longitude, along with measured data such as total precipitation, atmospheric pressure, global radiation, temperature, relative humidity, hourly wind direction, maximum wind gust and wind speed, all accompanied by date and time information. For the purposes of this study, specific data were extracted: date, time, global radiation (kJ/m^2) and wind speed (m/s).

For each basin of interest, a specific AMS was selected based on its data relevance. To determine the most suitable AMS, the correlation was calculated between the ENA data of each reservoir and the basin. The AMS located nearest to the reservoir and exhibiting the highest correlation coefficient with the reservoir's data was chosen as the representative station for that basin.

Data Adequacy and Processing

After selecting the AMS, it was necessary to conduct data quality control (QC) to identify potential suspicious or erroneous data and address it appropriately before proceeding with the analysis. It is commonplace for a dataset to exhibit some failures at some point, whether due to instrumental problems, registration errors or poor maintenance [47]. The QC procedure is summarized in Figure 1.

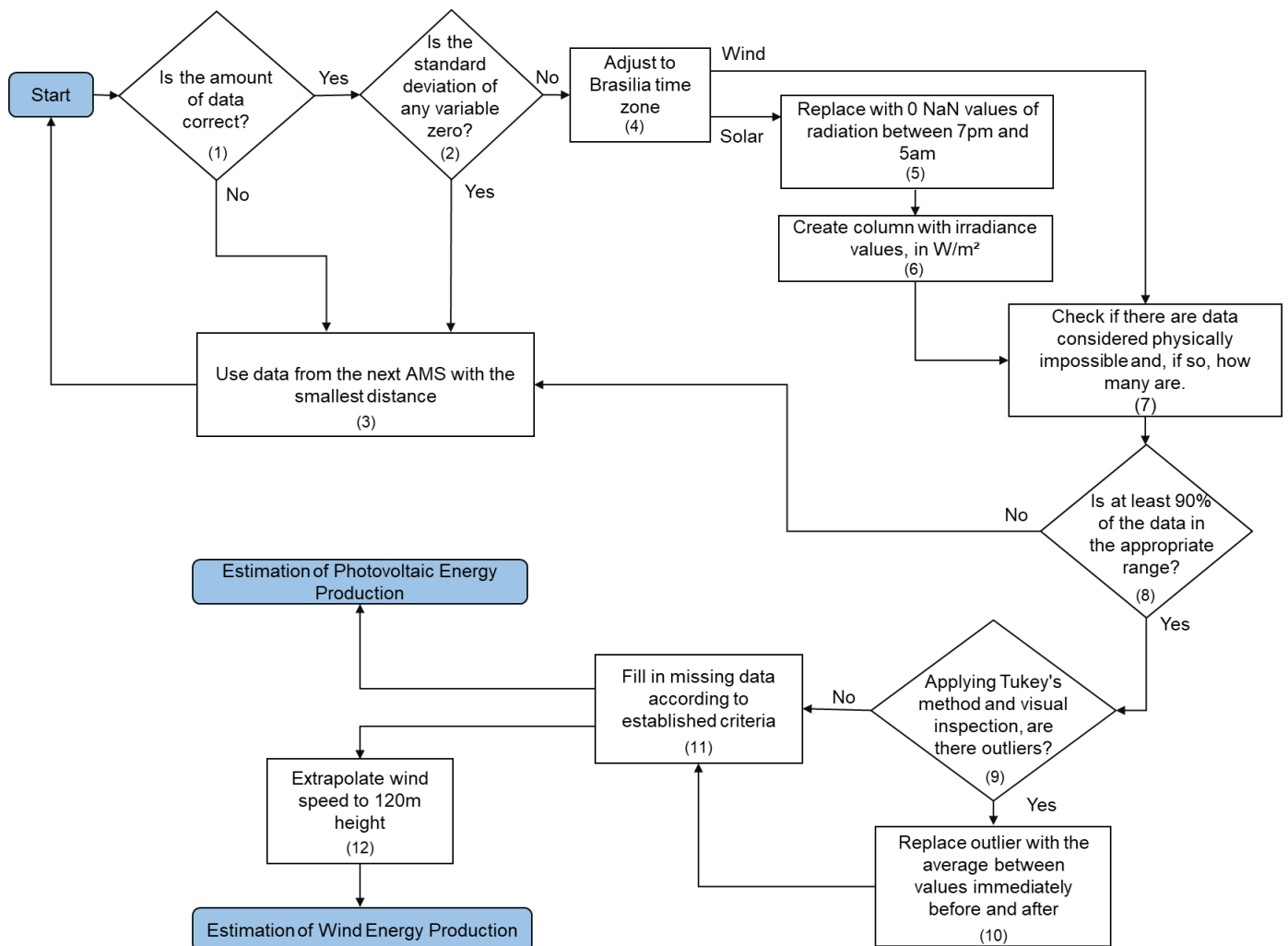


Figure 1. Data adequacy flowchart.

The quality control begins with the selection of the measurement file from the meteorological station nearest to the location of interest, the initial consideration focused on the number of lines and columns in the file. The correct values were 20 columns, due to the 19 distinct pieces of information available and the index column created by Python itself, and 8760 rows, considering that the files included hourly measurements for all 365 days of the year. For the year 2020, being a leap year, the expected number of rows was 8,784. If the

amount of data was incorrect, the subsequent station was chosen for analysis. In step 2, the standard deviation was calculated for each one of the data series. A null result would indicate that the equipment had not provided measurements correctly [48], i.e., all values are identical. In such cases, the measurement should be dismissed and step 3 is performed.

If the data number was correct, in step 4, the data were adjusted to the Brasília time zone because they were originally in Coordinated Universal Time (UTC), which is three hours ahead of Brasília time. It is crucial to acknowledge that Brazil encompasses four distinct time zones. The state of Paraná, the focus of this case study, adheres to the Brasília time zone, which is the standard time zone for the central and most populous regions of Brazil.

Regarding radiation, an additional adjustment was necessary: missing data, represented by NaN in Python, as well as data falling outside the time range of 6am to 6pm, were replaced with zero. This is because NaN indicates an absence of measurement, and outside this hourly interval, it is expected that the radiation will indeed be zero.

In the step 7 the process of checking the consistency of the radiation and wind speed data continues with a check for physically impossible values. The criteria used were the same as those adopted by the SONDA network (National Environmental Data Organization System), which is, in turn, based on two data quality control strategies: BSRN (Baseline Surface Radiation Network) and Webmet.com [49]. However, applying this criterion requires modifying the radiometric variable, as was done in Step 6.

In the case of the radiometric variable, although the term "global radiation" appears in the measurements provided by INMET, it is understood that the data actually represents horizontal global solar irradiance. This refers to the total rate of energy per unit area incident on a horizontal surface, in other words, the flow of solar radiation received [46,50]. As the data is available in kJ/m² and the samples are integrated into hourly values [51], it is possible to convert the unit using Equation 1:

$$\frac{kJ}{h.m^2} = \frac{1000 W}{3600 m^2} \quad (1)$$

A column was added to the data set with the values consistent with the established unit (W/m²). In general, negative values and those above the result of Equation 2 are considered physically impossible [49,52]. In this way, the upper limit is defined as:

$$Upper\ limit = S_a \cdot 1.5 \cdot \mu_0^{1,2} + 100 W/m^2 \quad (2)$$

Where:

$$S_a = \frac{S_0}{UA} \quad (3)$$

$$\mu_0 = \cos(\theta_z) \quad (4)$$

The solar constant adjusted for the Earth-Sun distance is denoted as S_a , UA is the Earth-Sun distance in Astronomical Units, S_0 is the solar constant at the average Earth-Sun distance, while θ_z represents the angle of the solar zenith.

Once all the physical limits had been established, the percentage of data within the appropriate range was investigated in step 8. If this value was less than 90% [53–55], the measurement would be discarded, and another AMS would need to be defined to represent the watershed. In all cases where the data from an AMS was not good enough for the analysis, the next AMS with the shortest distance from the HPP (hydroelectric power plant) would be selected and the entire process would be carried out again. In the event that the data outside the established limits represented less than 10% of the total, they would not be replaced or discarded.

In step 9, the presence of outliers in the measurements was evaluated. These values, which are discrepant from the rest of the dataset, deviate from the standard and can lead to calculation errors in statistical analyses and thereby potentially distorting conclusions and generalizations about the observed set [56].

Tukey's method was used to detect outliers. It is a methodology based on the IQR (interquartile range) widely used by researchers in the field of engineering in view of its simplicity, considerable effectiveness and ease of visualization and interpretation of the boxplot [57]. Furthermore, it is a method that does not assume distributional assumptions, nor does it depend on the mean or standard deviation, and should only be avoided in cases of small samples [58]. The values between the inner and outer fences are considered possible outliers, while a value that exceeds the outer fences is probably an outlier. The aforementioned values were

calculated for two distinct divisions of the dataset. In the initial analysis, all measurements for each variable throughout the year were considered, resulting in the identification of only two IQRs. In the second approach, the data for each variable were grouped by hour, resulting in 24 IQRs for each variable. In addition to employing the aforementioned method in its mathematical form, a visual analysis of the characteristic boxplots of the data was also conducted. Substitution would only be made if both the mathematical and visual criteria indicated inconsistent values, as indicated in step 10.

One of the difficulties in working with INMET data is the large amount of missing data, a challenge not unique to this system. Data incompleteness and the presence of unreliable data are intrinsic characteristics of the majority of available databases. In some cases, unreliable or missing data can account for up to 50% of entries [59]. One way around this problem is to exclude information containing missing data. However, this decision implies a reduction in sample size and could lead to the discarding of data that is useful for analysis, potentially resulting in a biased outcome. As a possible way to mitigate this issue, imputation methods have been developed to fill in the gaps with estimated values [60].

The fundamental concept of single imputation methods is a single value to replace each missing piece of information in the data set. There are several techniques based on this premise, including conditional mean imputation (CMI), where means are calculated for different subgroups based on the classification variables [59]. Missing data was then filled in step 11, following a priority and possibility order [59]:

- 1st: the result of the average between the values observed at that time on the previous day and the following day;
- 2nd: result of the average between the values of the previous and following hours;
- 3rd: result of the monthly average of the data measured at that time.

As this technique requires values from previous or following days, it is not applicable to the first and last days of the year. In the event of a gap occurring on these two days, the initial method to fill it was to use the average of the data from the hour before and the hour after the gap. Should this approach prove infeasible the gap would then be filled with the monthly average for the missing hour.

Finally, in order to estimate the photovoltaic energy generated, we considered a hypothetical 30 MW plant. The power of the photovoltaic array (P) was estimated using Equation 5.

$$P = \eta SG \quad (5)$$

In which η represents the total system efficiency, which was considered equal to 20%, S is the total area of photovoltaic module [m^2], considered equivalent to 150,000 m^2 and the global solar irradiance is G [W/m^2].

Regarding wind speed, an upper limit of 25 m/s was considered in step 7, as this restriction applies to measurements at 10 meters, the same height at which the AMSs collect data. The procedure outlined in steps 7 to 11 for solar data was similarly applied to the wind speed data.

After reviewing the data, we proceeded to extrapolate the wind speed data in step 12, keeping in consideration that the sensors capable of measuring wind speed, known as anemometers, are conventionally positioned 10 meters above the surface of the flat ground and in an open ground. The wind speed can be adjusted in relation to height using Equation 6, known as the logarithmic wind profile law, which is widely used across the European continent [61]. This law was also used in the development of the maps of different heights in the Atlas of Brazilian Wind Potential [62]; therefore, it was chosen for the extrapolation of speeds in this study.

$$\frac{v_2}{v_1} = \frac{\ln\left(\frac{h_2}{z_0}\right)}{\ln\left(\frac{h_1}{z_0}\right)} \quad (6)$$

The height from the ground at point 1 is denoted as h_1 , while the height of the ground at point 2 is h_2 . At point 1, the wind speed is v_1 . At point 2, it is v_2 . Finally, z_0 represents the roughness coefficient.

The roughness coefficient varies according to the region, since it corresponds to a measure in meters of the ground's imperfections [63]. In order to define the coefficient for each AMS, the digital elevation model was downloaded from INPE's TOPODATA project website [64]. The roughness layer was then opened in QGIS software, and the characteristic roughness values were identified using the latitude and longitude coordinates of the AMSs.

When it comes to generated wind power, estimates can be made using various models already proposed in the literature, including linear, exponential and cubic models. The last one was used in this work and is expressed according to Equation 7 [65].

$$P = n \frac{1}{2} C_p A \rho v_0^3 \quad (7)$$

P denotes the wind power and n represents the number of wind generators, while the power coefficient of wind generator is C_p , A is the area of the airstream, ρ is the air density in the local and the wind speed is v_0 .

In this model, with the exception of speed, all the terms can be considered constant and grouped together in a constant K. This means that the variation in the power of a wind turbine essentially depends on the cube of the speed at the specified height. Therefore, if complementarity is carried out in terms of generation, it is necessary to convert the wind speed series to wind speed cubed [21]. It is important to note that while the conversion of wind speed to wind speed cubed is essential for Pearson's correlation, it does not impact Spearman's rho and Kendall's tau, as these measures of correlation are based on rank order and are unaffected by the transformation. Furthermore, since K remains a constant multiplicative factor for all wind speed values, there will be no change in the result of the correlation coefficient calculation.

To estimate the wind power generated, wind speeds between 4 m/s and 25 m/s were considered, reflecting the current characteristics of wind turbines. For speed values outside this range, the power generated was considered null. For the purposes of this paper, a hypothetical wind farm of approximately 30 MW was considered, a value typically found in wind power plants. These include Tanque, Damascena and Maniçoba in the state of Bahia, Buriti, Nossa Senhora de Fátima and Itarema IX in the state of Ceará, Ventos de Santa Ângela 12, 19, 20 and 21 in Piauí, Santana I and Terral in Rio Grande do Norte, Coxilha Seca and Chuí V in Rio Grande do Sul and Salto and Bom Jardim in Santa Catarina [66]. The parameters used are shown in Table 1.

Table 1. Parameters used to estimate the wind power generated

Parameter	Value
Number of wind turbines – n	12
Power coefficient – C_p	0.42
Area of the airstream – A [m ²]	11,904.76
Air density – ρ [kg/m ³]	1.225

Once the generations had been estimated and the ENA data imported, the Kolmogorov-Smirnov test was applied to ascertain whether each of the data categories exhibited a normal distribution. Furthermore, the Harvey-Collier test was employed to assess linearity, while the Breusch-Pagan test was utilized to verify the homoscedasticity assumption. For all tests, the significance level (p-value) was set at 0.05. If the aforementioned assumptions were met, the Pearson coefficient would be employed to assess complementarity. In the event that the aforementioned tests did not yield satisfactory results, we employed the Mann-Kendall test to ascertain the monotonicity of the relationships between the data. Upon verifying monotonicity, the Spearman's Rho and Kendall's Tau coefficients would be employed. Opting for either of the latter two coefficient would suffice for assessing complementarity; however, one of the objectives of this article is to evaluate whether there exists a discrepancy between the results obtained in both coefficients.

Strategy for Complementarity Assessment

The complementarity assessment was conducted using results from correlation coefficients and the application of the Innovative Trend Analysis Methodology. In both approaches, the daily average values of photovoltaic and wind generation estimates, along with the daily values of ENA, were utilized. Although the data were daily, they were aggregated monthly for the calculation of correlation and ITA. The selection of the appropriate coefficient for each situation was based on the outcomes of normality, linearity, and homoscedasticity tests. If at least one variable failed to meet the assumptions required for the Pearson coefficient application, Spearman and Kendall coefficients were applied instead.

With regard to the correlation coefficient (r), the results obtained following the calculation for the hydraulic/photovoltaic and hydraulic/wind combinations should be interpreted in accordance with Table 2 [69], which presents the numerical ranges in absolute values. It is important to highlight that the response

obtained through the application of these metrics is dimensionless and varies from -1 to +1. Negative values indicate that the relationship between the observed variables is inversely proportional; as one increases, the other decreases. If the coefficient is zero, there is no correlation. Positive values denote the presence of a directly proportional correlation, indicating that the behaviors of the variables are similar, which can also be called similarity. The strength of the correlation increases as the absolute value of the coefficient approaches one, and weakens as it approaches zero [69]. The intermediate classification, which defines a correlation as weak or moderate, does not have precisely defined limits in the literature, but generally does not present significant variations.

Table 2. Interpretation of correlation coefficients values

Absolute value of the coefficient r	Correlation
$r \geq 0,9$	Very Strong
$0,7 \leq r < 0,9$	Strong
$0,4 \leq r < 0,7$	Moderate
$0,1 \leq r < 0,4$	Weak
$0,0 \leq r < 0,1$	Negligible

As the objective of the methodology was to evaluate complementarity, the best results would be the negative ones, particularly those closest to -1. This illustrates Since they would represent that, while one source produces the minimum, the other produces the maximum, ensuring that the demand continues to be met consistently.

With regard to the ITA method with significance test, the trend slope for each month is calculated in accordance with the methodology proposed in [40]. In the event that the value exceeds the upper (lower) confidence limit, it is accepted as an increasing (decreasing) trend. In the event that none of the mentioned conditions are met, it can be concluded that there is no statistically significant trend at a given confidence level [70]. This study employs a 95% confidence level. In instances where a declining trend is observed for one energy source while an increasing trend is observed for another, it can be posited that these sources exhibit complementarity.

RESULTS

Using the proposed methodology, the complementarity between two combinations of electrical energy sources was evaluated for the Capivari basin: hydraulic and photovoltaic and hydraulic and wind. These combinations of sources were chosen for two main reasons: firstly, because they include hydraulic generation, which still represents the largest portion of energy generation in Brazilian territory; secondly, because they offer viable options within the context of plant hybridization, especially in the case of photovoltaic generation with floating panels.

The chosen basin, located in the Brazilian state of Paraná, hosts a single hydroelectric plant along the course of its main river, Usina Capivari Cachoeira (Governador Pedro Viriato Perigot de Souza). Given the presence of only one HPP, the ENA of the reservoir is equivalent to the ENA of the basin. Consequently, the location of this reservoir is taken as the basis for analyzing the basin. According to the INMET data catalogue, the closest meteorological station to HPP Capivari Cachoeira, approximately 30 km away, was identified as "Barra do Turvo". However, this station did not fulfill the established data quality criteria. The subsequent closest AMS was "Morretes", also failed to meet the necessary standards for analysis. The third AMS, "Colombo", located 56 km from the HPP, satisfied the criteria set forth. This station, with data available from June 2016, enabled the monthly analysis spanning from that date to April 2024.

During this period, the data did not exhibit any outliers based on visual inspection, remaining within the expected value range; thus, there was no need for replacement. However, it was necessary to impute missing data according to the established criteria. The average percentage of imputed data per year was 8.51% for irradiance data and 3.61% for wind speed data. Over the entire period, 5,255 irradiance data points and 2,475 wind speed data points were imputed, representing approximately 7.58% and 3.57% of the total data, respectively.

When conducting the tests outlined in the methodology, the data did not exhibit a normal distribution, yet demonstrated a monotonicity. Therefore, the analyses were conducted using the Spearman and Kendall coefficients.

Complementarity analysis between photovoltaic and hydraulic generations using traditional methods

The results for Spearman's Rho and Kendall's Tau, which relate the photovoltaic and hydraulic generations for all months of the analyzed period, are presented in Table 3. Negative values of moderate and strong correlation are highlighted. The final line of the table presents the monthly average (Avg.) for each coefficient.

Table 3. Results obtained for the photovoltaic and hydraulic combination using traditional methods

Year	Coeff	Jan	Feb	Mar	Apr	May	Jun	Jul	Aug	Sep	Oct	Nov	Dec
2016	ρ_S	-	-	-	-	-	-0.54	-0.15	0.03	-0.35	-0.17	-0.10	-0.53
	τ	-	-	-	-	-	-0.40	-0.14	0.06	-0.23	-0.11	-0.09	-0.34
2017	ρ_S	-0.13	-0.49	0.11	-0.49	-0.28	-0.60	0.17	-0.48	-0.04	-0.02	0.34	-0.39
	τ	-0.09	-0.32	0.06	-0.34	-0.19	-0.44	0.14	-0.32	-0.03	-0.02	0.25	-0.29
2018	ρ_S	-0.10	-0.30	-0.37	-0.32	0.02	-0.58	0.12	-0.67	-0.06	0.09	0.15	-0.21
	τ	-0.09	-0.22	-0.28	-0.21	0.03	-0.46	0.08	-0.50	-0.03	0.05	0.08	-0.14
2019	ρ_S	-0.39	-0.41	-0.26	-0.41	-0.49	-0.11	-0.01	-0.09	-0.61	-0.10	-0.43	-0.61
	τ	-0.27	-0.27	-0.19	-0.29	-0.36	-0.09	0.00	-0.06	-0.44	-0.06	-0.28	-0.43
2020	ρ_S	-0.32	0.03	-0.14	-0.23	0.08	-0.47	-0.36	-0.54	-0.07	-0.24	-0.44	-0.40
	τ	-0.24	0.03	-0.07	-0.15	0.06	-0.35	-0.24	-0.35	-0.07	-0.15	-0.31	-0.28
2021	ρ_S	-0.34	-0.37	-0.24	0.37	-0.60	-0.31	0.21	-0.20	-0.31	-0.14	-0.56	-0.47
	τ	-0.25	-0.24	-0.15	0.21	-0.41	-0.19	0.16	-0.14	-0.21	-0.13	-0.34	-0.35
2022	ρ_S	-0.49	-0.06	-0.18	0.05	-0.66	-0.45	-0.09	-0.48	-0.06	-0.46	-0.57	-0.14
	τ	-0.36	0.01	-0.10	0.05	-0.49	-0.32	-0.03	-0.38	-0.04	-0.36	-0.40	-0.09
2023	ρ_S	-0.42	-0.19	-0.10	-0.45	-0.13	-0.70	-0.45	-0.61	-0.42	-0.35	0.00	0.15
	τ	-0.28	-0.12	-0.08	-0.32	-0.08	-0.54	-0.33	-0.43	-0.26	-0.27	0.03	0.14
2024	ρ_S	0.09	-0.22	0.32	-0.61	-	-	-	-	-	-	-	-
	τ	0.07	-0.16	0.22	-0.44	-	-	-	-	-	-	-	-
Avg.	ρ_S	-0.26	-0.25	-0.08	-0.26	-0.29	-0.53	-0.07	-0.48	-0.37	-0.17	-0.23	-0.33
	τ	-0.18	-0.15	-0.07	-0.19	-0.19	-0.47	-0.04	-0.27	-0.16	-0.16	-0.07	-0.22

Two of the twelve months of the year showed a negative correlation in all calculations made for the six years: June and September. Among them, June exhibited the highest average complementarity with a Spearman's Rho (ρ_S) of -0.53, followed by August with -0.48, which showed a negative correlation in all years except 2016. July, on the other hand, had the highest occurrence of positive correlation values, albeit weak, across the analyzed period, indicating similar generation patterns. Additionally, July also presents the lowest average monthly precipitation for the period of eight years, in comparison to the average of the other months [71]. Furthermore, it has the lowest average monthly ENA for the entire period, as illustrated in Figure 2. This suggests that energy generation planning could benefit from the existing complementarity, thereby prioritizing energy generation from one source over another during specific periods.

Comparing the results of the two coefficients, the behavior is quite similar, both present a negative correlation for most of the period, with the Spearman's Rho being a more favorable indicator of the correlation, due to the magnitude. The average of ρ_S , considering the 95 months of analysis, is -0.2505 and the average of τ is -0.177. Only in the month of February 2022, there is a discrepancy regarding the sign in the results. However, both results are considered negligible, which does not change the analysis as a whole.

Despite the average percentage difference between the mean coefficients being approximately 30%, only for the months of August and November does the interpretation of the results according to Table 2 change when analyzing both coefficients.

Complementarity analysis between wind and hydraulic generations using traditional methods

The outcomes for the Spearman's Rho and Kendall's Tau for, which depict the relationship between photovoltaic and hydraulic generations throughout all months within the scrutinized timeframe, are presented in Table 4. And negative values of moderate and strong correlations are emphasized.

Table 4. Results obtained for the wind and hydraulic combination using traditional methods

Year	Coeff	Jan	Feb	Mar	Apr	May	Jun	Jul	Aug	Sep	Oct	Nov	Dec
2016	ρ_S	-	-	-	-	-	-0.42	0.25	-0.09	-0.06	-0.16	0.09	0.08
	τ	-	-	-	-	-	-0.28	0.16	-0.05	-0.02	-0.12	0.06	0.07
2017	ρ_S	-0.15	0.12	-0.14	0.11	0.05	0.06	-0.03	0.11	-0.04	0.23	0.03	-0.10
	τ	-0.08	0.08	-0.12	0.07	0.04	0.03	-0.03	0.06	-0.01	0.13	0.03	-0.07
2018	ρ_S	-0.22	-0.28	-0.41	0.06	0.32	-0.51	-0.24	-0.53	0.15	0.09	0.05	0.22
	τ	-0.15	-0.18	-0.31	0.02	0.23	-0.35	-0.16	-0.37	0.10	0.08	0.03	0.13
2019	ρ_S	-0.33	-0.19	0.10	-0.39	0.01	-0.14	0.32	-0.31	-0.12	-0.14	0.05	-0.37
	τ	-0.23	-0.12	0.06	-0.25	0.00	-0.06	0.23	-0.24	-0.04	-0.09	0.03	-0.24
2020	ρ_S	-0.26	0.16	-0.24	-0.09	-0.28	-0.08	-0.18	0.07	-0.41	-0.19	-0.13	-0.44
	τ	-0.17	0.11	-0.19	-0.05	-0.18	-0.07	-0.13	0.05	-0.31	-0.12	-0.07	-0.30
2021	ρ_S	-0.05	-0.28	0.18	0.29	-0.20	-0.04	0.23	-0.03	0.09	-0.17	-0.54	-0.15
	τ	-0.07	-0.21	0.13	0.25	-0.12	-0.03	0.15	-0.03	0.07	-0.10	-0.44	-0.11
2022	ρ_S	-0.08	0.32	-0.37	-0.02	-0.25	-0.41	-0.17	0.04	-0.06	-0.37	-0.23	-0.18
	τ	-0.05	0.23	-0.27	0.02	-0.18	-0.28	-0.13	0.03	-0.05	-0.28	-0.18	-0.12
2023	ρ_S	0.04	0.38	0.09	-0.51	-0.07	-0.09	0.25	-0.03	0.15	0.27	0.03	-0.18
	τ	0.04	0.29	0.04	-0.39	-0.04	-0.08	0.14	-0.02	0.11	0.16	0.00	-0.11
2024	ρ_S	0.06	-0.03	0.39	-0.10	-	-	-	-	-	-	-	-
	τ	-0.08	0.01	0.10	-0.11	-	-	-	-	-	-	-	-
Avg.	ρ_S	-0.15	0.03	-0.05	-0.07	-0.06	-0.20	0.04	-0.10	-0.03	0.07	-0.08	-0.14
	τ	-0.10	0.00	-0.07	-0.06	-0.04	-0.13	0.02	-0.07	-0.02	-0.05	-0.07	-0.09

Approximately 61% of the acquired values were negative, a percentage lower than the over 82% observed for the photovoltaic and hydraulic combination. However, even though presenting negative values in more than half of the results, upon analyzing the monthly average values, we find that 8 are negligible and the remaining four indicate weak correlation. Regarding the utilization of the two coefficients, both illustrated

analogous trends, diverging solely in terms of sign for April 2022, and January and February 2024. Nonetheless, this discrepancy is irrelevant, given that all involved values are considered negligible. The average value of τ is approximately 49% lower than ρ_s . However, despite the considerable difference, the results of the two coefficients would have distinct interpretations only for the months of August and December, in which Spearman indicated the existence of weak correlation and Kendall indicated nonexistence.

Complementarity analysis using Innovative Trend Analysis

The calculated trend slope values are presented in Table 5. Values exceeding the confidence interval are indicated by a blue highlight, while values representing a significant decreasing trend are indicated by a yellow highlight. The remaining values do not indicate a significant trend.

Table 5. Results obtained using Innovative Trend Analysis

Year		Jan	Feb	Mar	Apr	May	Jun	Jul	Aug	Sep	Oct	Nov	Dec
2016	P _{PV}	-	-	-	-	-	-0.07	0.00	0.04	0.03	0.07	0.05	0.09
	P _W	-	-	-	-	-	-0.55	-2.35	0.76	-1.73	0.99	-0.53	0.43
	ENA	-	-	-	-	-	1.76	-0.92	10.0	-4.55	-0.54	0.09	-0.68
2017	P _{PV}	-0.14	0.12	-0.03	0.01	-0.09	0.03	0.05	0.01	-0.06	-0.08	0.01	-0.08
	P _W	-0.58	-0.67	-2.05	1.15	-0.12	-1.46	0.33	-1.78	-1.25	-1.01	0.81	1.16
	ENA	-0.89	-2.07	-0.25	-2.05	3.49	-7.74	0.20	1.01	0.72	-0.04	0.77	10.7
2018	P _{PV}	0.01	-0.01	-0.08	0.00	-0.01	0.09	-0.02	0.08	0.07	0.13	0.03	-0.06
	P _W	-0.80	0.22	-0.30	-0.97	0.48	-0.77	-0.01	0.99	0.59	0.31	1.71	-1.02
	ENA	6.95	-4.05	0.88	-0.48	-2.13	-1.28	0.47	-1.66	0.41	1.57	-2.32	-0.10
2019	P _{PV}	0.03	-0.08	-0.07	-0.05	-0.06	-0.02	0.02	-0.01	0.02	-0.04	0.16	0.19
	P _W	-1.40	1.02	-1.08	0.43	0.12	1.13	-0.09	-1.52	-0.26	0.07	-0.89	0.05
	ENA	2.08	5.96	1.14	-0.57	11.4	-8.39	-0.37	0.97	-0.13	-0.13	-1.36	-1.11
2020	P _{PV}	0.01	0.03	-0.04	-0.03	0.05	0.08	0.01	-0.06	0.00	-0.02	0.02	0.09
	P _W	1.05	0.05	0.36	-1.87	2.08	0.11	-1.39	-0.78	-0.15	-0.44	0.86	0.57
	ENA	-1.78	-1.29	-2.54	-0.16	0.09	0.08	-0.19	4.87	0.17	-0.95	-0.49	-1.41
2021	P _{PV}	-0.10	-0.04	-0.02	-0.06	0.03	-0.05	0.10	0.07	0.01	0.11	0.13	0.03
	P _W	1.02	-0.30	-1.55	-0.89	2.77	1.73	2.18	1.72	-0.96	-0.48	1.83	-0.04
	ENA	4.00	1.83	-5.66	-1.08	-0.59	1.97	0.55	-1.15	0.13	-0.06	-3.08	-0.10
2022	P _{PV}	0.15	0.00	-0.06	0.04	0.01	0.08	0.02	0.02	0.08	0.10	-0.04	-0.05
	P _W	0.40	0.02	1.24	0.81	1.70	2.37	-0.87	-0.26	-0.56	1.32	-0.66	-0.27
	ENA	2.13	-0.16	-0.76	0.02	0.77	-5.09	0.39	-1.14	1.31	1.45	16.9	-2.82
2023	P _{PV}	0.12	-0.14	0.10	-0.03	-0.06	0.02	-0.03	0.07	0.08	0.02	-0.20	0.05
	P _W	-0.88	0.31	-0.96	0.53	0.14	0.42	-1.45	1.76	-1.92	-0.31	0.14	0.52
	ENA	-3.07	-0.45	-2.05	-0.84	0.68	-0.74	0.16	-3.06	-0.16	-6.64	1.57	-1.67
2024	P _{PV}	-0.11	-0.19	-0.06	0.07	-	-	-	-	-	-	-	-
	P _W	-0.77	-1.10	0.04	0.87	-	-	-	-	-	-	-	-
	ENA	-3.07	-0.81	-2.41	-1.09	-	-	-	-	-	-	-	-

The significant values in Table 5 indicate that in 17 months, the trends in photovoltaic generation (P_{PV}) and hydraulic generation, represented by ENA, are opposite. This indicates that while one source of generation increases, the other decreases, thereby characterizing complementarity. Of these 17 values, 11 months coincide with the months showing moderate correlation according to Table 3. The remaining six months correspond to months exhibiting weak correlation.

With regard to the combination of wind generation (P_w) and hydraulic generation, 13 months indicate complementarity between the sources. Among these months, three have a moderate correlation coefficient, as indicated in Table 4. Six months have a weak correlation coefficient, while four months exhibit a positive or negligible correlation.

DISCUSSION

With the application of the methodology, it was possible to notice that the data did not present a normal distribution as expected. Consequently, one of the main assumptions for using Pearson's linear correlation coefficient was not met, indicating that the Pearson coefficient should not be used. This finding challenges the approach of most complementarity studies carried out in Brazil and around the world, which utilize this coefficient without acknowledging any specific knowledge about the distribution of data. However, the paper [24] demonstrates similar results for the application of Spearman and Pearson coefficients in an analysis between wind and hydraulic generation sources for the Brazilian territory. In article [72], the author opts for the Kendall's Tau as an indicator of complementarity because the data did not follow a normal distribution. However, he included in the research a comparison between the results obtained using the Pearson coefficient, Spearman's Rho and Kendall's Tau. According to the author, the three indicators exhibit similar tendency. Nevertheless, the Pearson coefficient exhibits a higher range than Kendall's Tau, while the Spearman's Rho shows a wider range than Kendall's Tau and a similar range as the Pearson coefficient.

It is worth noting that mathematical analyses available in the literature [31,73,74] indicate that the magnitudes of Kendall's results are expected to be lower than those of Spearman's. This is consistent with the findings obtained in this study. Additionally, in [75], different possible cutoff values are proposed compared to those used in this work. This is because the values of τ are lower than the coefficients of Pearson and Spearman for the same strength. According to this proposition, values are considered weak from 0.06, moderate from 0.026, strong from 0.49, and very strong above 0.71.

In terms of numerical findings, the study conducted by [24], evaluated the correlation between wind and hydraulic generations and the authors mention weak complementarity in the state of Paraná as one of the results, with a correlation coefficient within the range of -0.3 to 0. This is consistent with what was found in the current research, where the average of ρ_s , considering the 95 months of analysis, is -0.071 and the average of τ is -0.053, both falling within the mentioned range. Comparing this result with those of other studies carried out in other locations in the Brazilian territory demonstrates the climatic diversity found in Brazil and reinforces the idiosyncrasy of the Brazilian power system. Consider, for instance, the outcomes reported in [15], where a correlation coefficient exceeding 0.6 was estimated in an analysis spanning from 1948 to 2010 for the northeast region of Brazil. And also the correlation maps presented in [14] which indicate high potential for complementarity in 50% of the territory occupied by the Brazilian state of Rio Grande do Sul.

The research conducted by [26] assessed the complementarity among hydraulic, wind, and photovoltaic generations in Brazil, employing a methodology that divided the country into regions based on the annual behavior of each energy resource, a practice previously employed in [76,77]. Complementarities were analyzed between the same source in different regions, between different sources within the same region, and between different sources across different regions. Although, the regions studied are significantly larger in size than the Capivari basin. For comparison purposes, the basin was considered part of the regions designated as H1, W2 and S1 in the related work. The results obtained indicated a correlation of 0.92 for the wind-hydraulic combination and -0.47 for the photovoltaic-hydraulic combination. Unlike the first combination, which showed high similarity, the second combination's results suggest a moderate level of complementarity.

Figure 2 presents normalized monthly averages of ENA, photovoltaic generation, and wind generation over the analyzed period. The blue line indicates that hydropower generation is typically lower during the autumn and winter periods in the region, spanning from the end of March to the end of September. This period could thus be advantageous for supplementing demand with alternative energy sources even if the correlation is not considered strong. By comparing the mathematically obtained results for complementarity with those shown in the figure, wind generation could complement demand in June, while photovoltaic generation could support the remainder of the period with lower hydropower generation.

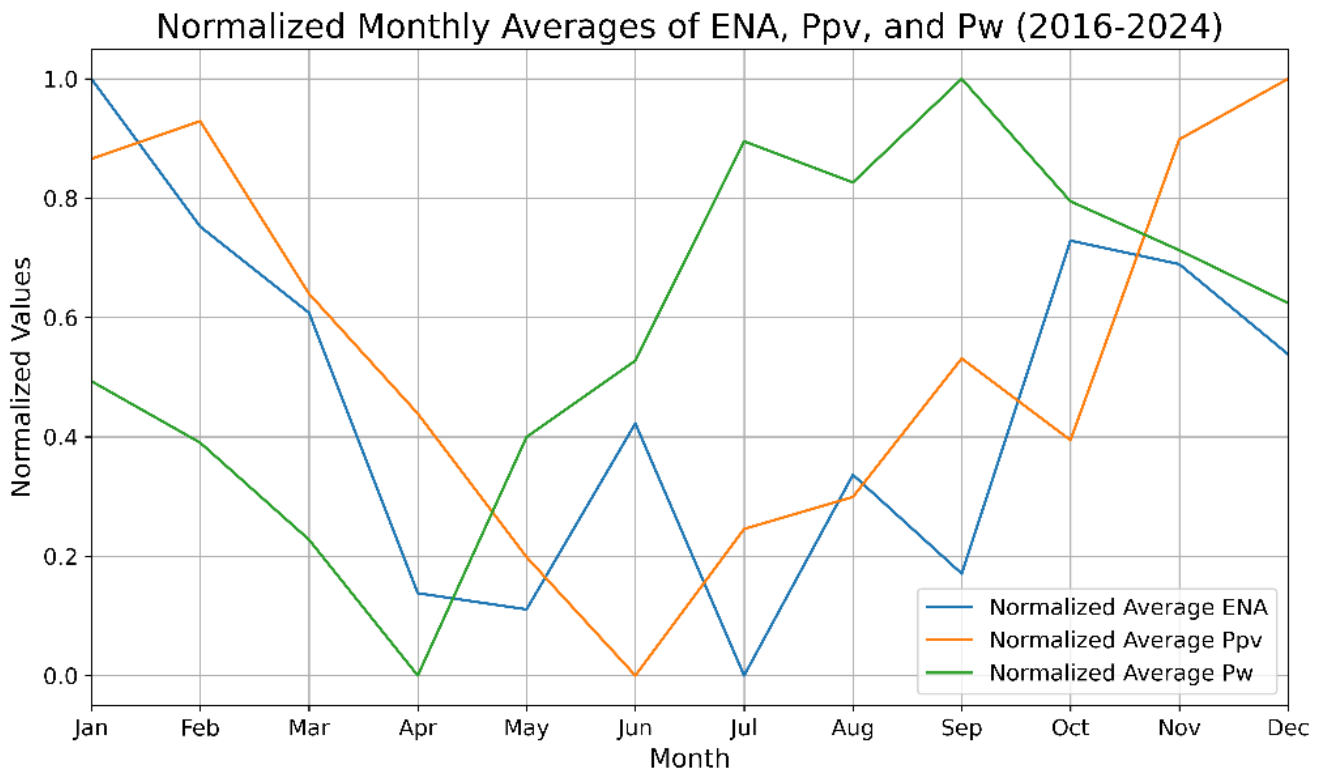


Figure 2. Monthly Averages of Hydroelectric, Photovoltaic, and Wind Generation.

CONCLUSION

The purpose of the developed methodology is to enable its replication for the analysis of any river basin in Brazil. This article is confined to the territory of Brazil, with limitations imposed by the use of databases sourced exclusively from institutions within the country. Given that the developed procedure can be easily adapted with minimal modifications for application in other geographical locations, the outcomes derived from employing this methodology have the potential to serve as a valuable tool for contributing to energy generation planning. This is particularly relevant in the context of hybrid plant configurations, aiming to enhance the efficient utilization of existing infrastructures and optimize investments in new resources, such as energy storage systems and floating photovoltaic panels.

When applying the Capivari basin as a case study for the methodology, it was observed that the results obtained for the Kendall and Spearman coefficients were quite similar. However, it was noted that Kendall's tau was approximately 30% lower than Spearman's rho when considering the monthly averages of the photovoltaic and hydraulic combination, and 49% lower when considering the combination of wind and hydraulic. Despite these discrepancies in magnitude, the analysis regarding the presence or absence of complementarity derived from both coefficients remained consistent. The combination of photovoltaic and hydroelectric generations was found to be more attractive than the combination of wind and hydroelectric, as it exhibited correlations ranging from weak to strong in approximately 72% of the months, according to Spearman's correlation coefficient observation. In contrast, the index for the latter combination was found to be around 44%. The responses obtained with the ITA also support this perception, as the number of months showing opposite trends for the combination involving photovoltaic generation is approximately 23.5% higher than the number of months involving wind generation.

In essence, the findings extend beyond the specific context of the Capivari basin, presenting a methodology that not only contributes to the efficient use of existing infrastructures but also serves as tool to optimize investments in new resources, such as energy storage systems and floating photovoltaics panels. The implications reach beyond national borders, providing a versatile framework poised to shape the future of energy planning on a broader scale.

Funding: This research was funded by Conselho Nacional de Desenvolvimento Científico (CNPq).

Conflicts of Interest: The authors declare no conflict of interest.

REFERENCES

1. Jurasz J, Canales FA, Kies A, Guezgouz M, Beluco A. A review on the complementarity of renewable energy sources: Concept, metrics, application and future research directions. *Sol Energy* [Internet]. 2020 [cited 2024 Jul 25];195(October 2019):703–24. Available from: <https://doi.org/10.1016/j.solener.2019.11.087>
2. Ren G, Liu J, Wan J, Guo Y, Yu D. Overview of wind power intermittency: Impacts, measurements, and mitigation solutions. *Appl Energy* [Internet]. 2017 [cited 2024 Jul 25];204:47–65. Available from: <http://dx.doi.org/10.1016/j.apenergy.2017.06.098>
3. Jacobson MZ, Delucchi MA. Providing all global energy with wind, water, and solar power, Part I: Technologies, energy resources, quantities and areas of infrastructure, and materials. *Energy Policy* [Internet]. 2011 [cited 2024 Jul 25]; 39(3):1154–69. Available from: <http://dx.doi.org/10.1016/j.enpol.2010.11.040>
4. Dias CO. [Study and computational implementation of an energy storage system with direct connection to the electrical system] [dissertation]. Uberlândia: Universidade Federal de Uberlândia; 2020 [cited 2024 Jul 25]. 166 p. Available from: <https://repositorio.ufu.br/handle/123456789/28777>
5. Beluco A, Krenzinger A, Souza P. A. [The Temporal Complementarity between Hydroelectric and Photovoltaic Energies]. *Rev Bras Recur Hídricos*. 2003;8(1):99–109.
6. Fernandes PC, Risso A, Beluco A. A survey on temporal and spatial complementarity between wind and solar resources along the coast of northeastern Brazil. In: Jurasz J, Beluco A, editors. *Complementarity of Variable Renewable Energy Sources*. Elsevier; 2022. p. 99–120.
7. Cantão MP. [Hydro-wind Complementarity in the Brazilian Territory]. 2015 [cited 2024 Jul 24]. Available from: <https://tecnologia.ufpr.br/ppgerha/wp-content/uploads/sites/9/2015/02/RelatorioComplementaridadeHidroolica.pdf>
8. Stiubiener U, Carneiro ST, Trigo FB, Benedito RS, Teixeira JC. PV power generation on hydro dam's reservoirs in Brazil: A way to improve operational flexibility. *Renew Energy* [Internet]. 2020 [cited 2024 Jul 25];150:765–76. Available from: <https://doi.org/10.1016/j.renene.2020.01.003>
9. Galdino M, Oliveri M. [Considerations on the implementation of floating photovoltaic systems in Brazil]. In: VI Congresso Brasileiro de Energia Solar [Internet]. Belo Horizonte-MG; 2016 [cited 2024 Jul 25]. p. 1–6. Available from: <http://www.abens.org.br/CBENS2016/anais/anais/trabalhos/2538Ofinal.pdf>
10. Ceribasi G, Caliskan M. Short- and long-term prediction of energy to be produced in hydroelectric energy plants of Sakarya Basin in Turkey. *Energy Sources, Part A Recover Util Environ Eff* [Internet]. 2023 [cited 2024 Jul 25];45(1):2680–95. Available from: <https://doi.org/10.1080/15567036.2019.1665756>
11. Dos Anjos PS, Da Silva AS, Stošić B, Stošić T. Long-term correlations and cross-correlations in wind speed and solar radiation temporal series from Fernando de Noronha Island, Brazil. *Phys A Stat Mech its Appl* [Internet]. 2015 [cited 2024 Jul 25];424:90–6. Available from: <http://dx.doi.org/10.1016/j.physa.2015.01.003>
12. Campos RA, do Nascimento LR, Rütther R. The complementary nature between wind and photovoltaic generation in Brazil and the role of energy storage in utility-scale hybrid power plants. *Energy Convers Manag* [Internet]. 2020 [cited 2024 Jul 25];221(April):113160. Available from: <https://doi.org/10.1016/j.enconman.2020.113160>
13. Braga NB, Barbosa AL, Borba BS, Silva NV, Mattos RL. [Analysis of the regions of Bahia with the highest potential for hybridization of wind-photovoltaic plants, considering the transmission system margin]. In: XXVI Seminário Nacional de Produção e Transmissão de Energia Elétrica (SNPTEE). Rio de Janeiro; 2022.
14. Bagatini M, Benevit MG, Beluco A, Risso A. Complementarity in Time between Hydro, Wind and Solar Energy Resources in the State of Rio Grande do Sul, in Southern Brazil. *Energy Power Eng*. 2017;09(09):515–26.
15. Ricosti JF, Sauer IL. An assessment of wind power prospects in the Brazilian hydrothermal system. *Renew Sustain Energy Rev*. 2013;19:742–53.
16. Weschenfelder F. Impact of climate change on wind and solar energy sources complementarity: a case study of the northeast Brazilian region. In: Jurasz J, Beluco A, editors. *Complementarity of Variable Renewable Energy Sources*. Elsevier; 2022. p. 243–69.
17. Neto PB, Saavedra OR, Oliveira DQ. The effect of complementarity between solar, wind and tidal energy in isolated hybrid microgrids. *Renew Energy* [Internet]. 2020 [cited 2024 Jul 25];147:339–55. Available from: <https://doi.org/10.1016/j.renene.2019.08.134>
18. MME/EPE. [Generation expansion planning studies - Evaluation of the generation of hybrid wind-photovoltaic plants: Methodological proposal and case studies] [Internet]. 2017 [cited 2024 Jul 25]. p. 32. Available from: [https://www.epe.gov.br/sites-pt/publicacoes-dados-abertos/publicacoes/PublicacoesArquivos/publicacao-232/topico-214/Metodologia para avaliação de usinas híbridas eólico-fotovoltaicas.pdf](https://www.epe.gov.br/sites-pt/publicacoes-dados-abertos/publicacoes/PublicacoesArquivos/publicacao-232/topico-214/Metodologia%20para%20avaliacao%20de%20usinas%20hibridas%20eolico-fotovoltaicas.pdf)
19. Rosa CO, Costa KA, Christo ES, Bertahone PB. Complementarity of hydro, photovoltaic, and wind power in Rio de Janeiro State. *Sustain*. 2017;9(7):1–12.
20. Rosa CO. [Complementarity study between hydroelectric, wind and photovoltaic energy in the Southeast and Central-West regions] [dissertation]. Volta Redonda: Universidade Federal Fluminense; 2019 [cited 2024 Jul 25]. 159 p. Available from: <http://mcct.uff.br/wp-content/uploads/sites/454/2019/10/Disserta%C3%A7%C3%A3o-Caroline-de-Oliveira-defendeu-em-25-02-2019.pdf>
21. Rezende BR. [Complementarity between renewable sources through Principal Component Analysis] [dissertation]. Volta Redonda: Universidade Federal Fluminense; 2020 [cited 2024 Jul 25]. 92 f. Available from: <http://mcct.uff.br/wp-content/uploads/sites/454/2021/09/Disserta%C3%A7%C3%A3o-B%C3%A1rbara-Raquel-defendeu-em-25-09-2020.pdf>

22. ONS. [SIN Electric Energy Matrix] [Internet]. 2023 [cited 2023 Jun 6]. Available from: <https://www.ons.org.br/paginas/sobre-o-sin/o-sistema-em-numeros>
23. Gallardo RP. A comparative study of correlation coefficients used to assess the solar and wind complementarity in Mexico. In: Jurasz J, Beluco A, editors. *Complementarity of Variable Renewable Energy Sources*. Elsevier; 2022. p. 269–90.
24. Canales FA, Acuña GJ. Metrics and indices used for the evaluation of energetic complementarity—a review. In: Jurasz J, Beluco A, editors. *Complementarity of Variable Renewable Energy Sources*. Elsevier; 2022. p. 35–55.
25. Cantão MP, Bessa MR, Bettega R, Detzel DHM, Lima JM. Evaluation of hydro-wind complementarity in the Brazilian territory by means of correlation maps. *Renew Energy*. 2017;101:1215–25.
26. Bett PE, Thornton HE. The climatological relationships between wind and solar energy supply in Britain. *Renew Energy* [Internet]. 2016;87:96–110. Available from: <http://dx.doi.org/10.1016/j.renene.2015.10.006>
27. Aza-Gnandji M, Fifatin FX, Hounnou AH, Dubas F, Chamagne D, Espanet C, et al. Complementarity between Solar and Wind Energy Potentials in Benin Republic. *Adv Eng Forum* [Internet]. 27 de junho de 2018;28:128–38. Available from: <https://www.scientific.net/AEF.28.128>
28. Paredes JR, Ramírez JJ. Variable Renewable Energies and Their Contribution to Energy Security: Complementarity in Colombia. *Inter-American Dev Bank Energy Div*. 2017;57.
29. da Luz TJ, Vila CU, Aoki AR. Complementarity Between Renewable Energy Sources and Regions - Brazilian Case. *Brazilian Arch Biol Technol* [Internet]. 2023;66. Available from: http://www.scielo.br/scielo.php?script=sci_arttext&pid=S1516-89132023000100609&lng=en
30. Kougiass I, Szabó S, Monforti-Ferrario F, Huld T, Bódis K. A methodology for optimization of the complementarity between small-hydropower plants and solar PV systems. *Renew Energy*. 2016;87:1023–30.
31. Silva AR, Pimenta FM, Assireu AT, Spyrides MH. Complementarity of Brazil's hydro and offshore wind power. *Renew Sustain Energy Rev*. 2016;56:413–27.
32. Jurasz J, Beluco A, Canales FA. The impact of complementarity on power supply reliability of small scale hybrid energy systems. *Energy*. 2018;161:737–43.
33. Croux C, Dehon C. Influence functions of the Spearman and Kendall correlation measures. *Stat Methods Appl*. 2010;19(4):497–515. doi:10.1007/s10260-010-0142-z.
34. Kirch W. Pearson's Correlation Coefficient. In: *Encyclopedia of Public Health* [Internet]. Dordrecht: Springer Netherlands; 2008. Available from: https://link.springer.com/10.1007/978-1-4020-5614-7_2569
35. El-Hashash EF, Shiekh RH. A Comparison of the Pearson, Spearman Rank and Kendall Tau Correlation Coefficients Using Quantitative Variables. *Asian J Probab Stat*. 2022;(November):36–48.
36. Hodge VJ, Austin JI. A Survey of Outlier Detection Methodologies. *Artif Intell Rev*. 2004;22:85–126.
37. Pir H, Ceribasi G, Ceyhunlu AI. The effect of climate change on energy generated at hydroelectric power plants: A case of Sakarya river basin in Turkey. *Renew Energy* [Internet]. 2024 [cited 2024 Aug 2];223:120077. Available from: <https://linkinghub.elsevier.com/retrieve/pii/S0960148124001423>
38. Ceribasi G, Ceyhunlu AI, Wałęga A, Młyński D. Investigation of the Effect of Climate Change on Energy Produced by Hydroelectric Power Plants (HEPPs) by Trend Analysis Method: A Case Study for Dogancay I–II HEPPs. *Energies*. 2022;15(7).
39. Ali R, Kuriqi A, Abubaker S, Kisi O. Long-term trends and seasonality detection of the observed flow in Yangtze River using Mann-Kendall and Sen's innovative trend method. *Water (Switzerland)*. 2019;11(9).
40. Pessoa JO, Lima AM, Junior JC, Dos Santos EM, Pessoa JO, de Oliveira LM, et al. Application of the Innovative Trend Analysis (ITA) Method for detecting trends in annual and seasonal rainfall in the Metropolitan Region of Recife. *Rev Bras Geogr Fis*. 2023;16(6):2958–77.
41. Esit M. Investigation of innovative trend approaches (Ita with significance test and ipt) comparing to the classical trend method of monthly and annual hydrometeorological variables: A case study of Ankara region, Turkey. *J Water Clim Chang*. 2023;14(1):305–29.
42. Şen Z. Innovative trend significance test and applications. *Theor Appl Climatol*. 2017;127(3–4):939–47.
43. TIOBE Software. TIOBE Index for July 2024 [Internet]. 2024 [cited 2024 Aug 2]. Available from: <https://www.tiobe.com/tiobe-index/>
44. Branco DC. [What was the most popular programming language of 2021?] [Internet]. Canaltech. 2022 [cited 2024 Aug 2]. Available from: <https://canaltech.com.br/seguranca/qual-foi-a-linguagem-de-programacao-mais-popular-de-2021-205993/>
45. INMET. BDMEP – [Historical Data] [Internet]. [cited 2024 Aug 2]. Available from: <https://portal.inmet.gov.br/servicos/bdmep-dados-historicos>
46. Pereira E, Martins F, Gonçalves A, Costa R, Lima F, Rütther R, et al. Brazilian solar energy atlas [Internet]. São José dos Campos, SP; 2017 [cited 2024 Aug 02]. 80 p. Available from: <http://urlib.net/rep/8JMKD3MGP3W34P/3PERDJE>
47. Cantor D, Mesa O, Ochoa A. Complementarity beyond correlation. In: Jurasz J, Beluco A, editors. *Complementarity of Variable Renewable Energy Sources*. Elsevier; 2022. p. 121–41.
48. Relva SG. [Irradiation characterization method for photovoltaic generation: a systemic analysis of primary energy modeling] [dissertation]. São Paulo: Universidade de São Paulo; 2017 [cited 2024 Aug 2] 269 p. Available from: <https://teses.usp.br/teses/disponiveis/3/3143/tde-17032017-141345/pt-br.php>

49. INPE. SONDA – Data validation [Internet]. 2021 [cited 2024 Aug 2]. Available from: <http://sonda.ccst.inpe.br/infos/validacao.html>
50. de Oliveira AS. [Chapter IV – Solar radiation] [Internet]. UFRB. [cited 2024 Aug 2]. p. 10. Available from: <https://www.ufrb.edu.br/neas/documento/category/8-cca-035-meteorologia-e-climatologia-agricola?download=40:cap-4-radsolar>
51. INMET. [Technical note 001/2011SEGER/LAIME/CSC/INMET - INMET Automatic Meteorological Stations Network]. 2011 [cited 2024 Aug 2]. p. 1–11. Available from: https://www.cemtec.ms.gov.br/wp-content/uploads/2019/02/Nota_Tecnica-Rede_estacoes_INMET.pdf
52. Moreno-Tejera S, Ramírez-Santigosa L, Silva-Pérez MA. A proposed methodology for quick assessment of timestamp and quality control results of solar radiation data. *Renew Energy*. 2015;78:531–7.
53. Rosa CO, Christo ES, Costa KA, Santos L. Assessing complementarity and optimising the combination of intermittent renewable energy sources using ground measurements. *J Clean Prod* [Internet]. 2020;258:120946. Available from: <https://doi.org/10.1016/j.jclepro.2020.120946>
54. Portmann RW, Solomon S, Hegerl GC. Spatial and seasonal patterns in climate change, temperatures, and precipitation across the United States. *Proc Natl Acad Sci U S A*. 2009;106(18):7324–9.
55. Ntsangwane L, Mabasa B, Sivakumar V, Zwane N, Ncongwane K, Botai J. Quality control of solar radiation data within the South African Weather Service solar radiometric network. *J Energy South Africa*. 2019;30(4):51–63.
56. Lima LF, Maroldi AM, da Silva DVO, Hayashi MCPI, Hayashi CRM. [Outlier detection in scientific metrics: preliminary study for univariate data]. In: 5th Brazilian Meeting of Bibliometrics and Scientometrics [Internet]. São Paulo; 2016 [cited 2024 Aug 2]. p. A21–31. Available from: <https://brapci.inf.br/index.php/res/download/55785>
57. Dastjerdy B, Saeidi A, Heidarzadeh S. Review of Applicable Outlier Detection Methods to Treat Geomechanical Data. *Geotechnics*. 2023;3(2):375–96.
58. Seo S. A review and comparison of methods for detecting outliers in univariate data sets [Internet]. University of Pittsburgh; 2006 [cited 2024 Aug 2]. Available from: <http://d-scholarship.pitt.edu/7948/>
59. Veroneze R. Tratamento de Dados Faltantes Empregando Biclusterização com Imputação Múltipla. Campinas: Universidade Estadual de Campinas [dissertation]; 2011 [cited 2024 Aug 2]. 238 p. Available from: https://www.dca.fee.unicamp.br/~vonzuben/theses/dissertacao_Rosana_Veroneze.pdf
60. Stochero EL. [The influence of data variability on the imputation quality of missing data]. Santa Maria: Universidade Federal de Santa Maria; 2019 [cited 2024 Aug 2]. 60 p. Available from: The influence of data variability on the imputation quality of missing data
61. CEPEL (BR). [Reference Manual - NEWAVE Model] [Internet]. 2012 [cited 2024 Aug 2]. p. 106. Available from: https://simsee.org/simsee/biblioteca/Brasil/NW201203/ManualReferencia_Newave_comentado.pdf
62. CEPEL (BR). [Atlas of Brazilian Wind Potential - Simulations 2013] [Internet]. 2017 [cited 2024 Aug 2]. p. 52. Available from: <http://novoatlas.cepel.br/>
63. Prado PO. [Design of a wind farm using a geographic information system] [dissertation]. Guaratinguetá: Universidade Estadual Paulista; 2009 [cited 2024 Aug 2]. 90 p. Available from: https://repositorio.unesp.br/bitstream/handle/11449/99280/prado_po_me_guara.pdf?sequence=1&isAllowed=y
64. INPE. Topodata - Map Index [Internet]. [cited 2024 Aug 2]. Available from: <http://www.dsr.inpe.br/topodata/acesso.php>
65. Kishore GR, Prema V, Rao KU. Multivariate wind power forecast using artificial neural network. 2014 IEEE Glob Humanit Technol Conf - South Asia Satell GHTC-SAS 2014. 2014;159–63.
66. ONS (BR). Plant List Table [Internet]. [cited 2024 Aug 2]. Available from: <https://www.ons.org.br/Paginas/resultados-da-operacao/historico-da-operacao/tabela-relacao-usinas.aspx>
67. Dufour JM. Recursive stability analysis of linear regression relationships - An Exploratory Methodology. *J Econom*. 1982;19:31–76.
68. Williams R. Heteroskedasticity [Internet]. University of Notre Dame; 2020 [cited 2024 Aug 2]. p. 1–16. Available from: <https://www3.nd.edu/~rwilliam/stats2/I25.pdf>
69. Schober P, Schwarte LA. Correlation coefficients: Appropriate use and interpretation. *Anesth Analg*. 2018;126(5):1763–8.
70. Şan M, Akçay F, Linh NT, Kankal M, Pham QB. Innovative and polygonal trend analyses applications for rainfall data in Vietnam. *Theor Appl Climatol*. 2021;144(3–4):809–22.
71. Instituto das Águas do Paraná (BR). [Monthly precipitation heights (mm)] [Internet]. 2023 [cited 2024 Aug 2]. Available from: <http://www.sih-web.aguasparana.pr.gov.br/sih-web/gerarRelatorioAlturasMensaisPrecipitacao.do?action=carregarInterfaceInicial>
72. Kapica J. Global complementarity of renewable energy sources. . In: Jurasz J, Beluco A, editors. *Complementarity of Variable Renewable Energy Sources*. Elsevier; 2022. p. 141–70.
73. Fredricks GA, Nelsen RB. On the relationship between Spearman's rho and Kendall's tau for pairs of continuous random variables. *J Stat Plan Inference*. 2007 [cited 2024 Aug 2];137:2143-2150. Available from: <https://doi.org/10.1016/j.jspi.2006.06.045>
74. Capéraà P, Genesr C. Spearman's ρ is larger than Kendall's τ for positively dependent random variables. *J Nonparametr Stat*. 1993; 2:183-94.

75. Wicklin R. Weak or strong? How to interpret a Spearman or Kendall correlation. 2023 Apr 5 [cited 2024 Aug 2]. In: SAS Blogs, c2024. Available from: <https://blogs.sas.com/content/iml/2023/04/05/interpret-spearman-kendall-corr.html>.
76. Da Luz T, Moura P. Power generation expansion planning with complementarity between renewable sources and regions for 100% renewable energy systems. *Int Trans Electr Energy Syst*. 2019;29(7):1–19.
77. Da Luz T, Moura P. 100% Renewable energy planning with complementarity and flexibility based on a multi-objective assessment. *Appl Energy* [Internet]. 2019 [cited 2024 Aug 2];255(August):113819. Available from: <https://doi.org/10.1016/j.apenergy.2019.113819>



© 2024 by the authors. Submitted for possible open access publication under the terms and conditions of the Creative Commons Attribution (CC BY) license (<https://creativecommons.org/licenses/by/4.0/>)